

# Lattice study of vacuum polarization function and determination of strong coupling constant

E. Shintani,<sup>1,\*</sup> S. Aoki,<sup>2</sup> T. W. Chiu,<sup>3</sup> S. Hashimoto,<sup>1,4</sup> T. H. Hsieh,<sup>5</sup>  
T. Kaneko,<sup>1,4</sup> H. Matsufuru,<sup>1</sup> J. Noaki,<sup>1</sup> T. Onogi,<sup>6</sup> and N. Yamada<sup>1,4</sup>

(JLQCD and TWQCD collaboration)

<sup>1</sup>*High Energy Accelerator Research Organization (KEK), Tsukuba 305-0801, Japan*

<sup>2</sup>*Graduate School of Pure and Applied Sciences,  
University of Tsukuba, Tsukuba 305-8571, Japan*

<sup>3</sup>*Physics Department, Center for Theoretical Sciences,  
and National Center for Theoretical Sciences,  
National Taiwan University, Taipei 10617, Taiwan*

<sup>4</sup>*School of High Energy Accelerator Science,  
The Graduate University for Advanced Studies (Sokendai), Tsukuba 305-0801, Japan*

<sup>5</sup>*Research Center for Applied Sciences,  
Academia Sinica, Taipei 115, Taiwan*

<sup>6</sup>*Yukawa Institute for Theoretical Physics,  
Kyoto University, Kyoto 606-8502, Japan*

## Abstract

We calculate the vacuum polarization functions on the lattice using the overlap fermion formulation. By matching the lattice data at large momentum scales with the perturbative expansion supplemented by Operator Product Expansion (OPE), we extract the strong coupling constant  $\alpha_s(\mu)$  in two-flavor QCD as  $\Lambda_{\overline{MS}}^{(2)} = 0.234(9)_{-0}^{+16}$  GeV, where the errors are statistical and systematic, respectively. In addition, from the analysis of the difference between the vector and axial-vector channels, we obtain some of the four-quark condensates.

PACS numbers: 11.15.Ha,12.38.Gc,12.38.Aw

---

\*Electronic address: shintani@post.kek.jp

## I. INTRODUCTION

In Quantum Chromodynamics (QCD) the vacuum polarization, defined through the (axial-)vector current correlator, contains rich information of its perturbative and non-perturbative dynamics. In the long distance regime it is sensitive to the low-lying particle spectrum. The short distance regime, on the other hand, can be analyzed using perturbation theory supplemented by the Operator Product Expansion (OPE). The current correlator can be expressed as an expansion in terms of the strong coupling constant  $\alpha_s$  together with power corrections of the form  $\langle \mathcal{O}^{(n)} \rangle / Q^n$ . Here, the local operator  $\mathcal{O}^{(n)}$  has a mass dimension  $n$  and  $Q$  is the momentum scale flowing into the correlator. Determination of  $\alpha_s$  (and of the vacuum expectation values  $\langle \mathcal{O}^{(n)} \rangle$ , in principle) can be performed by applying the formulae for experimental results of  $e^+e^-$  cross section or  $\tau$  decay distributions [1], for instance. On the other hand, if one can *calculate* the correlators non-perturbatively, theoretical determination of those fundamental parameters is made possible.

Lattice QCD calculation offers such a non-perturbative technique. Two-point correlators can be calculated for space-like separations. In this work we investigate the use of the perturbative formulae of the correlators for the lattice data obtained in the high  $Q^2$  regime. The strong coupling constant  $\alpha_s$  may then be extracted. In such an analysis, it is essential to find the region of  $Q^2$  where the perturbative expression can be applied and at the same time the discretization error is under control. By inspecting the numerical data, we find that this is indeed possible at a lattice spacing  $a \simeq 0.12$  fm if we subtract the bulk of the discretization effects non-perturbatively. The remaining effect can be estimated using the perturbation theory.

The idea of analyzing the short distance regime is not new: in fact, the analysis of hadron correlators in the whole length-scales was proposed 15 year ago [2], but to our knowledge quantitative analysis including the determination of  $\alpha_s$  and  $\langle \mathcal{O}^{(n)} \rangle$  has been missing until recently. (Calculation of the vacuum polarization from the vector current correlator in lattice QCD may be found in [3, 4]. More recently, an analysis of charmonium correlator has been published [5].)

While the vacuum polarizations  $\Pi_J(Q^2)$  ( $J$  denotes vector or axial-vector channel) are ultraviolet divergent and their precise value depends on the renormalization scheme, their derivative  $D_J(Q^2) = -Q^2 d\Pi_J(Q^2)/dQ^2$ , called the Adler function [6], is finite and renormal-

ization scheme independent. Therefore, the continuum perturbative expansion of  $D_J(Q^2)$  to order  $\alpha_s^3$  [7, 8], can be directly applied to the lattice data. At relatively low  $Q^2$  region, higher order terms of OPE become relevant. They include the parameters describing the gluon condensate  $\langle\alpha_s G^2\rangle$  and the quark condensate  $\langle m\bar{q}q\rangle$  (we suppress quark flavor index assuming degenerate up and down quark masses) at  $O(1/Q^4)$ , and four-quark condensates  $\langle O_8\rangle$  and  $\langle O_1\rangle$  at  $O(1/Q^6)$  [9, 10]. (The explicit form of  $O_8$  and  $O_1$  will be given in Section III B.)

We use the lattice QCD data containing two dynamical flavors described by the overlap fermions [11]. The simulations are performed at lattice spacing  $a = 0.118(2)$  fm on a  $16^3 \times 32$  lattice. For the details of the simulation including the choice of the lattice actions and parameters, we refer [11]. The physical volume is about  $(1.9 \text{ fm})^3$ , which is relatively small compared to the present large scale QCD simulations. The finite volume effect is, however, not significant for the short distance quantities considered in this work. The quark masses  $m_q$  in this analysis are 0.015, 0.025, 0.035 and 0.050 in the lattice unit, that cover the range  $[m_s/6, m_s/2]$  with  $m_s$  the physical strange quark mass. An analysis of pion mass and decay constant is presented in [12].

The main advantage of this data set is that both the sea and valence quarks preserve exact chiral and flavor symmetries by the use of the overlap fermion formulation [13, 14]. (Although the fermionic currents used in our calculation are not conserved at finite lattice spacings, it does not change the following argument of the operator mixing.) The perturbative formulae for the vacuum polarizations can therefore be applied without any modification due to explicit violation of the chiral symmetry. For instance, the scalar density operator  $\bar{q}q$  to define the quark condensate is free from the leading power divergence which scales as  $1/a^3$ . This means that a term of the form  $ma^{-3}/Q^4$  is forbidden in the OPE formula as in the continuum theory. With the Wilson-type fermion formulation, this term may appear and has to be identified and subtracted non-perturbatively. With the staggered fermion formulation, there is no such problem because of its remnant chiral symmetry, while the effect of taste-breaking may become significant when  $(aQ)^2$  becomes  $O(1)$ .

This paper is organized as follows. In Section II we define the vacuum polarization functions and explain the method to calculate them on the lattice. Subtraction of lattice artifacts is discussed in some detail. Section III summarizes the perturbative formulae of OPE. Then, in Section IV we show the results of fitting of our data with the perturbative formulae. Estimate of the systematic errors is also given. Conclusions are given in Section V.

## II. VACUUM POLARIZATION FUNCTION

### A. Definition

In the continuum theory, the vacuum polarization functions  $\Pi_J^{(\ell)}(Q^2)$  are defined through two-point correlation functions as

$$\begin{aligned} \langle J_\mu J_\nu \rangle(Q) &\equiv \int d^4x e^{iQ \cdot x} \langle T \{ J_\mu^{ij}(x) J_\nu^{ji}(0) \} \rangle \\ &= (\delta_{\mu\nu} Q^2 - Q_\mu Q_\nu) \Pi_J^{(1)}(Q^2) - Q_\mu Q_\nu \Pi_J^{(0)}(Q^2), \end{aligned} \quad (1)$$

where the current  $J_\mu^{ij}$  may either be a vector current  $V_\mu^{ij} = \bar{q}_i \gamma_\mu q_j$  or an axial-vector current  $A_\mu^{ij} = \bar{q}_i \gamma_\mu \gamma_5 q_j$  with flavor indices  $i \neq j$ .  $\Pi_J^{(1)}(Q^2)$  and  $\Pi_J^{(0)}(Q^2)$  denote the transverse and longitudinal parts of the vacuum polarization, respectively. For the vector channel ( $J = V$ ),  $\Pi_V^{(0)}(Q^2) = 0$  is satisfied due to current conservation. For the axial-vector channel ( $J = A$ ), the longitudinal component may appear when the quark mass is finite.

In the lattice calculation we employ the overlap fermion formulation [13, 14], for which the Dirac operator is given by

$$D(m) = \left( m_0 + \frac{m}{2} \right) + \left( m_0 - \frac{m}{2} \right) \gamma_5 \text{sgn} [H_W(-m_0)] \quad (2)$$

for a bare quark mass  $m$ . The kernel operator  $H_W(-m_0) \equiv \gamma_5 D_W(-m_0)$  is constructed from the conventional Wilson-Dirac operator  $D_W(-m_0)$  at a large negative mass  $-m_0$ . We set  $m_0 = 1.6$  in the numerical simulation. We use the vector and axial-current operators of the form

$$V_\mu^{ij} = Z \bar{q}_i \gamma_\mu \left( 1 - \frac{D}{2m_0} \right) q_j, \quad (3)$$

$$A_\mu^{ij} = Z \bar{q}_i \gamma_\mu \gamma_5 \left( 1 - \frac{D}{2m_0} \right) q_j. \quad (4)$$

With this choice, the vector and axial charges form a multiplet under the axial transformation  $\delta_A^a q_i = \varepsilon \tau_{ij}^a \gamma_5 (1 - D/m_0) q_j$ ,  $\delta_A^a \bar{q}_i = \varepsilon \bar{q}_j \tau_{ji}^a \gamma_5$ , where  $\varepsilon$  denotes an infinitesimal parameter and  $\tau^a$  is a generator of the flavor  $SU(2)$  symmetry. The overlap fermion action is invariant under this modified chiral transformation [15], as it satisfies the Ginsparg-Wilson relation  $D\gamma_5 + \gamma_5 D = D\gamma_5 D/m_0$  [16]. The common renormalization factor  $Z$  has been calculated non-perturbatively as  $Z = 1.3842(3)$  [12].

An obvious drawback of the (axial-)vector currents in (3) and (4) is that the current conservation property  $\partial_\mu J_\mu = 0$  ( $J = V$  or  $A$ ) is not satisfied at finite lattice spacing. It leads to a significant complication in the extraction of the functions  $\Pi_J^{(0)}(Q^2)$  and  $\Pi_J^{(1)}(Q^2)$ , as described in the next subsection. The use of the conserved (axial-)vector current [17] reduces this complication. Once we have extracted the functions  $\Pi_J^{(0)}(Q^2)$  and  $\Pi_J^{(1)}(Q^2)$ , these two types of currents should give an equally good approximation to the continuum one up to the unphysical constant shift (and the discretization error). Our preliminary study employing the conserved currents shows that this is indeed the case.

## B. Non-perturbative subtraction of lattice artifact

Due to the discretization effects including the current non-conservation effect, the two-point correlation functions (1) may have more complicated structures. Taking account of remaining symmetries on the lattice (parity and cubic symmetries) but without the current conservation, the correlators on the lattice  $\langle J_\mu J_\nu \rangle^{\text{lat}}(Q)$  can be expressed as an expansion in  $Q_\mu$ :

$$\begin{aligned} \langle J_\mu J_\nu \rangle^{\text{lat}}(Q) &= \Pi_J^{(1)}(Q) Q^2 \delta_{\mu\nu} - \Pi_J^{(0+1)}(Q) Q_\mu Q_\nu \\ &- \sum_{n=0}^{\infty} B_n^J(Q) Q_\mu^{2n} \delta_{\mu\nu} - \sum_{m,n=1}^{\infty} C_{mn}^J(Q) \{ Q_\mu^{2m+1} Q_\nu^{2n-1} + Q_\nu^{2m+1} Q_\mu^{2n-1} \}, \end{aligned} \quad (5)$$

in the momentum space. The lattice momentum  $Q_\mu$  is defined as  $Q_\mu = (2/a) \sin(\pi n_\mu / L_\mu)$  with an integer four-vector  $n_\mu$  whose components take values in  $(-L_\mu/2, L_\mu/2]$  on a lattice of size  $L_\mu$  in the  $\mu$ -th direction ( $L_{i=1,2,3} = 16$  and  $L_t = 32$  in our case). The functions corresponding to the continuum counterparts,  $\Pi_J^{(1)}(Q)$  and  $\Pi_J^{(0+1)}(Q)$  ( $\equiv \Pi_J^{(0)}(Q) + \Pi_J^{(1)}(Q)$ ), may also have Lorentz-violating effects and could be a function of  $Q_\mu$  in general rather than a function of just a single argument  $Q^2$ .

The term  $B_0^J(Q) \delta_{\mu\nu}$ , which has the same Lorentz structure as the term of physical  $\Pi_J^{(1)}(Q)$  does, contains a quadratically divergent contact term. Since one cannot disentangle the physical contribution from the unphysical divergence using the Lorentz structure alone, we focus on extracting  $\Pi_J^{(0+1)}(Q)$ , which is free from the contact term.

The terms including functions  $B_{n>0}^J(Q)$  and  $C_{mn}^J(Q)$  represent the lattice artifacts that violate the Lorentz symmetry. They are generally written in terms of an expansion in  $aQ_\mu$  and  $aQ_\nu$ . (Physically relevant terms are separately written with a conventional notation

$\Pi_J^{(1)}(Q)$  and  $\Pi_J^{(0+1)}(Q)$ .) The lowest order term  $B_1^J(Q)$  remains constant in the continuum limit  $aQ \rightarrow 0$ , while the terms of  $B_2^J(Q)$  and  $C_{11}^J(Q)$  are relatively suppressed by  $O((aQ)^2)$  and vanish in the continuum limit. Higher order terms are suppressed by additional powers of  $a$  at a fixed  $Q$ . Since the momentum scale  $Q$  of interest is not much less than the lattice cutoff  $1/a$ , the convergence of the expansion at our lattice spacing must be carefully investigated for the lattice data. These terms can be identified non-perturbatively, and we found that the lowest non-trivial terms including  $B_2^J(Q)$  and  $C_{11}^J(Q)$  are already very small as described below. Higher order terms are thus safely neglected.

Extraction of  $B_{1,2}^J(Q)$  and  $C_{11}^J(Q)$  from the lattice data goes as follows. The off-diagonal components  $\langle J_\mu J_\nu \rangle^{\text{lat}}(Q)$  ( $\mu \neq \nu$ ) contain  $\Pi_J^{(0+1)}(Q)$  and  $C_{11}^J(Q)$ , hence by taking the data with two different momentum configurations giving the same  $Q^2$  one can solve a linear equation to disentangle  $\Pi_J^{(0+1)}(Q)$  from the lattice artifact. To be explicit, for two different momentum configurations  $aQ^{(1)}$  and  $aQ^{(2)}$  giving the same  $(aQ^{(1)})^2 = (aQ^{(2)})^2 = (aQ)^2$ , the linear equation is written as

$$\begin{aligned} \langle J_\mu J_\nu \rangle^{\text{lat}}|_{\mu \neq \nu}(Q^{(1)}) &= aQ_\mu^{(1)} aQ_\nu^{(1)} \Pi_J^{(0+1)}(Q^{(1)}) - (aQ_\mu^{(1)}(aQ_\nu^{(1)})^3 + aQ_\nu^{(1)}(aQ_\mu^{(1)})^3) C_{11}^J(Q^{(1)}), \\ \langle J_\mu J_\nu \rangle^{\text{lat}}|_{\mu \neq \nu}(Q^{(2)}) &= aQ_\mu^{(2)} aQ_\nu^{(2)} \Pi_J^{(0+1)}(Q^{(2)}) - (aQ_\mu^{(2)}(aQ_\nu^{(2)})^3 + aQ_\nu^{(2)}(aQ_\mu^{(2)})^3) C_{11}^J(Q^{(2)}). \end{aligned} \quad (6)$$

We may assume the equalities  $\Pi_J^{(0+1)}(Q^{(1)}) = \Pi_J^{(0+1)}(Q^{(2)})$  and  $C_{11}^J(Q^{(1)}) = C_{11}^J(Q^{(2)})$  for small enough  $(aQ)^2$ , because  $aQ^{(1)}$  and  $aQ^{(2)}$  are different only by permutations of space-time directions. The linear equation (6) can be solved when

$$Q_\mu^{(1)} Q_\nu^{(1)} Q_\mu^{(2)} Q_\nu^{(2)} [(Q_\mu^{(2)})^2 + (Q_\nu^{(2)})^2 - (Q_\mu^{(1)})^2 - (Q_\nu^{(1)})^2] \neq 0. \quad (7)$$

It is easy to see that three different non-zero components must be contained in  $aQ^{(1)}$  and  $aQ^{(2)}$  to satisfy (7). The smallest possible momentum assignment corresponds to the combination  $|n_\mu^{(1)}| = (2, 1, 0, 1)$ ,  $|n_\mu^{(2)}| = (1, 2, 0, 1)$  with  $(\mu, \nu) = (1, 4)$  and its permutations. Since the fourth (temporal) direction is longer for our lattice ( $L_{i=1,2,3} = 16$  while  $L_4 = 32$ ), the fourth component of  $Q_\mu$  is effectively 1/2 of spatial components when they are the same in  $n_\mu$ . The corresponding momentum squared for this choice is  $(aQ)^2 \simeq 0.776$ . For larger lattice momenta, there are many possible choices that this procedure is applied.

The lattice artifact in the diagonal pieces,  $B_1^J(Q)$  and  $B_2^J(Q)$ , can be extracted in a similar manner by solving linear equations for  $\mu = \nu$  after subtracting the  $C_{11}^J(Q)$  terms.

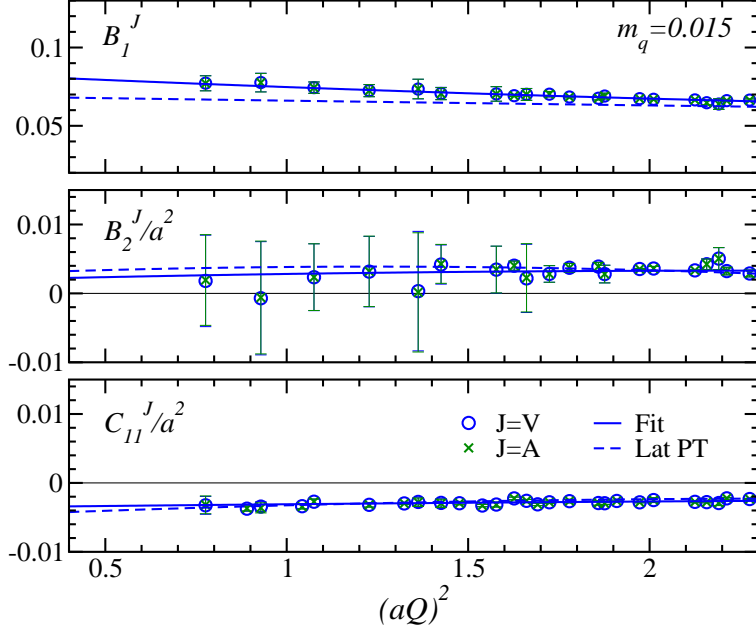


FIG. 1: Momentum dependence of  $B_1^J(Q)$ ,  $B_2^J(Q)/a^2$ , and  $C_{11}^J(Q)/a^2$  at  $m_q = 0.015$ . Circles (crosses) show the vector (axial-vector) channel. The solid curves represent a polynomial fit and the dashed curves show the one-loop results.

For instance, the leading contribution  $(\Pi_J^{(1)}(Q)Q^2 - B_0^J(Q))\delta_{\mu\nu}$  is extracted by subtracting the sub-leading contribution  $B_1^J(Q)Q_\mu^2\delta_{\mu\nu}$ , which can be identified from a difference between  $\langle J_1 J_1 \rangle^{\text{lat}}(Q)$  and  $\langle J_2 J_2 \rangle^{\text{lat}}(Q)$  at the same  $Q^2$ , for instance.

Figure 1 shows the numerical results for  $B_1^J(Q)$ ,  $B_2^J(Q)/a^2$  and  $C_{11}^J(Q)/a^2$  at the smallest quark mass ( $m_q = 0.015$ ) as a function of  $(aQ)^2$  for both vector and axial channels. In the momentum region  $(aQ)^2 < 2.3$  only the  $B_1^J(Q)$  term gives sizable contribution, while the others are an order of magnitude smaller even without the suppression due to  $(aQ)^2$ . Their dependence on  $(aQ)^2$  is rather mild, so that it seems reasonable to fit these functions as a polynomial of  $(aQ)^2$ . We use a third-order polynomial to model these functions. This is used to subtract the artifacts at the momentum points for which the above procedure is not applicable, *e.g.* below the lowest  $(aQ)^2 \simeq 0.776$ .

We notice that the difference between  $J = V$  and  $J = A$  is consistent with zero within statistical errors. This indicates that these lattice artifacts are strongly constrained by the exact chiral symmetry of the overlap fermion, and the effect of the finite quark mass is negligible. It also suggests that such short distance quantities are insensitive to the

spontaneous chiral symmetry breaking, as it should be. This property is essential in the calculation of the difference  $\Pi_V^{(\ell)}(Q) - \Pi_A^{(\ell)}(Q)$ , which is related to the electromagnetic mass difference of pions [18, 19].

### C. Perturbative calculation of the lattice artifacts

Since the lattice artifacts are most significant in the high  $(aQ)^2$  region, perturbative analysis of the discretization effects is expected to give a reasonable estimate. We calculate the vacuum polarization functions in the lattice perturbation theory at one-loop level, which means that only the zeroth order of  $\alpha_s$  is included. We then extract the terms corresponding to  $\Pi_J^{(0+1)}(Q)$ ,  $B_{1,2}^J(Q)$  and  $C_{11}^J(Q)$ .

We calculate the vacuum polarization diagram in which two (axial-)vector currents (3) and (4) are inserted. The renormalization factor  $Z$  is set equal to 1 at this order. In the momentum space, the two-point function is written as

$$\begin{aligned} \langle V_\mu V_\nu \rangle^{\text{lat}}(Q) &= \int_{-\pi}^{\pi} \frac{d^4 K}{(2\pi)^4} \text{Tr} \left[ \left( 1 - \frac{1}{2m_0} D_0(K) \right) S_0(K) \gamma_\mu \right. \\ &\quad \left. \times \left( 1 - \frac{1}{2m_0} D_0(K - Q) \right) S_0(K - Q) \gamma_\nu \right], \end{aligned} \quad (8)$$

where the fermion propagator  $S_0(K)$  is given by

$$S_0(K) = \frac{1}{2m_0} \left[ \frac{-i \sum_\mu \gamma_\mu \sin(K_\mu)}{\omega(K) + b(K)} + 1 \right] \quad (9)$$

with

$$\omega(K) = \sqrt{\sum_\mu \sin^2(K_\mu) + b(K)^2}, \quad (10)$$

$$b(K) = \sum_\mu (1 - \cos(K_\mu)) - m_0 \quad (11)$$

for the overlap fermion and  $D_0(K)^{-1} = S_0(K)$ . We set  $a = 1$  in this subsection. In the perturbative calculation,  $m_0$  may be set equal to 1. At the perturbative level, the vector and axial-vector current correlators are equivalent in the massless limit, because of the exact chiral symmetry of the overlap fermion.

After performing the numerical integral in (8) we extract  $B_{1,2}(Q)$ ,  $C_{11}(Q)$  and  $\Pi_V(Q)$  in (5) through the same numerical procedure as we used in the non-perturbative extraction. To be explicit, we take representative values of  $(aQ)^2$  between 0.4 and 2.3 and



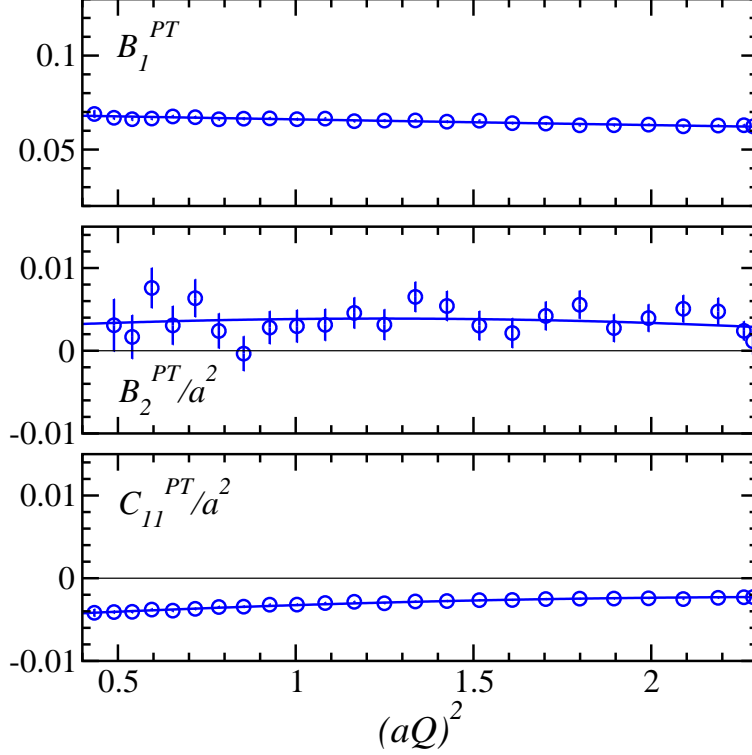


FIG. 2: Momentum dependence of  $B_1^J(Q)$ ,  $C_{11}^J(Q)/a^2$  and  $B_2^J(Q)/a^2$  calculated in perturbation theory.

consider two different momentum configurations  $aQ^{(1)}$  and  $aQ^{(2)}$ . The results for  $B_1(Q)$ ,  $B_2(Q)/a^2$ , and  $C_{11}(Q)/a^2$  are shown in Figure 2. As we found in the non-perturbative calculation, the  $(aQ)^2$  dependence is rather mild and we may precisely model these functions by quadratic functions:  $B_1^{PT}(Q) = 0.06930(59) - 0.00332(85)(aQ)^2 + 0.00009(27)(aQ)^4$ ,  $B_2^{PT}(Q) = 0.0025(22) + 0.0023(30)(aQ)^2 - 0.0009(9)(aQ)^4$ , and  $C_{11}^{PT}(Q) = -0.00507(14) + 0.00227(20)(aQ)^2 - 0.00046(6)(aQ)^4$ . The fit curves are shown in Figure 2.

The same curves are also plotted in Figure 1 by dashed lines. These perturbative results show reasonable agreement with the lattice data. It indicates that the lattice artifacts are indeed well described by the perturbation theory.

#### D. Results for the vacuum polarization functions

Lattice results for the vacuum polarization function  $\Pi_J^{(0+1)}(Q)$  for  $J = V$  are shown in Figure 3. The vacuum polarization function can be extracted from off-diagonal  $\mu \neq \nu$

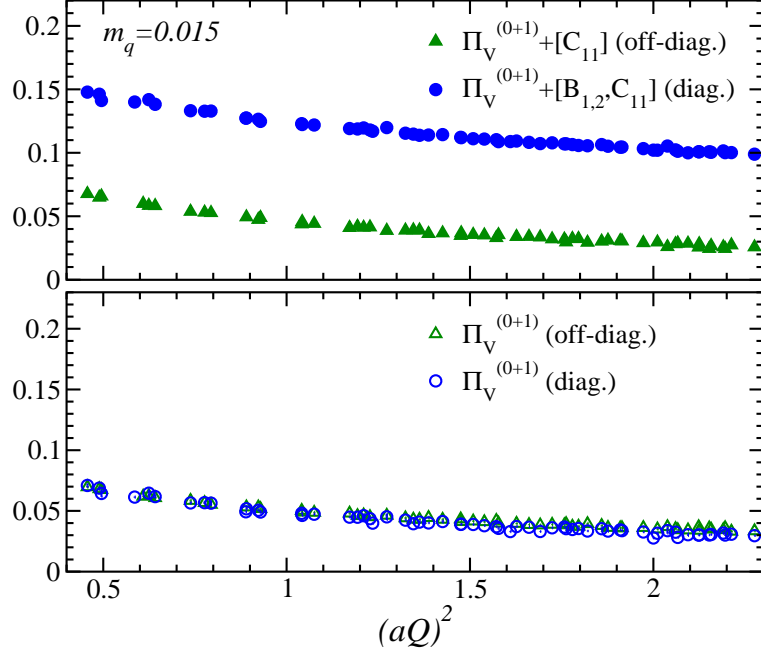


FIG. 3:  $\Pi_V^{(0+1)}(Q)$  from off-diagonal  $\mu \neq \nu$  and diagonal  $\mu = \nu$  correlators with (lower panel) and without (upper panel) the subtraction of  $B_{1,2}^J(Q)$  and  $C_{11}^J(Q)$ .

(triangles) and from diagonal  $\mu = \nu$  (circles) components. Upper and lower panels show the data before and after the subtraction of  $B_n^J(Q)$  and  $C_{mn}^J(Q)$  terms. Namely, for the upper panel,  $\Pi_V^{(0+1)}(Q)$  is identified with the formula (5) but without the  $B_n^J(Q)$  and  $C_{mn}^J(Q)$  terms. As discussed above, raw lattice data of the diagonal components receive large contamination from  $B_1^J(Q)$  while the artifact for the off-diagonal components is much smaller (below 0.01).

After the non-perturbative subtraction of  $B_{1,2}^J(Q)$  and  $C_{11}^J(Q)$ , we observe that the off-diagonal and diagonal components give consistent results. It strongly indicates that the higher order lattice artifacts are unimportant. We average the diagonal and off-diagonal data in the following analysis.

### III. OPERATOR PRODUCT EXPANSION

#### A. $V$ and $A$ channels

We now discuss the fit of the lattice data to the OPE expression of the form [20]

$$\begin{aligned} \Pi_J^{(0+1)} \Big|_{\text{OPE}}(Q^2) = & c + C_0(Q^2, \mu^2) + \frac{m^2}{Q^2} C_m^J(Q^2, \mu^2) + C_{\bar{q}q}^J(Q^2) \frac{\langle m\bar{q}q \rangle}{Q^4} \\ & + C_{GG}(Q^2) \frac{\langle (\alpha_s/\pi) GG \rangle}{Q^4}. \end{aligned} \quad (12)$$

Instead of directly treating the Adler function, we analyze its indefinite integral  $\Pi_J^{(0+1)} \Big|_{\text{OPE}}(Q^2)$ . The coefficient functions  $C_0(Q^2, \mu^2)$ ,  $C_m^J(Q^2, \mu^2)$ ,  $C_{\bar{q}q}^J(Q^2)$  and  $C_{GG}(Q^2)$  are analytically calculated in perturbation theory. The terms of order  $1/Q^6$  and higher are not included.

A constant  $c$  is divergent and thus scheme-dependent, while other terms are finite and well-defined. Although we need to specify the renormalization scheme, the scheme dependence should disappear as the higher order terms are included. The following formulae are consistently given in the  $\overline{\text{MS}}$  scheme, so that the strong coupling constant  $\alpha_s(\mu)$  is defined in this conventional scheme.

The leading term  $C_0(Q^2, \mu^2)$  is known to  $\mathcal{O}(\alpha_s^2)$  in the massless limit [7, 8] as

$$\begin{aligned} C_0(Q^2, \mu^2) = & \frac{1}{16\pi^2} \left\{ \frac{20}{3} + 4 \ln \frac{\mu^2}{Q^2} + \frac{\alpha_s(\mu^2)}{\pi} \left[ \frac{55}{3} - 16\zeta(3) + 4 \ln \frac{\mu^2}{Q^2} \right] \right. \\ & + \left( \frac{\alpha_s(\mu^2)}{\pi} \right)^2 \left[ \frac{41927}{216} - \frac{3701}{324} N_f - \left( \frac{1658}{9} - \frac{76}{9} N_f \right) \zeta(3) + \frac{100}{3} \zeta(5) \right. \\ & \left. \left. + \left\{ \frac{365}{6} - \frac{11}{3} N_f - \left( 44 - \frac{8}{3} N_f \right) \zeta(3) + \left( \frac{11}{2} - \frac{1}{3} N_f \right) \ln \frac{\mu^2}{Q^2} \right\} \ln \frac{\mu^2}{Q^2} \right] \right\}, \end{aligned} \quad (13)$$

where  $N_f$  denotes the number of flavors, and the zeta function is numerically given as  $\zeta(3) = 1.20205\dots$ ,  $\zeta(5) = 1.03692\dots$ . For a finite quark mass there is a contribution of  $\mathcal{O}(m^2/Q^2)$  with running mass  $m = m(\mu)$ . This term is represented by  $C_m^J(Q^2, \mu^2)$ , which is

also calculated to  $\mathcal{O}(\alpha_s^2)$  as

$$\begin{aligned}
C_m^V(Q^2, \mu^2) &= \frac{1}{4\pi^2} \left[ -6 + \frac{\alpha_s(\mu^2)}{\pi} \left( -16 - 12 \ln \frac{\mu^2}{Q^2} \right) \right. \\
&\quad + \left( \frac{\alpha_s(\mu^2)}{\pi} \right)^2 \left\{ -\frac{19691}{72} + \frac{95}{12} N_f - \frac{124}{9} \zeta(3) + \frac{1045}{9} \zeta(5) \right. \\
&\quad \left. - \left( 55 + 12 \ln \frac{\mu^2}{Q^2} \right) \ln \frac{\mu^2}{Q^2} - \left( 11 - \frac{2}{3} N_f \right) \left( \frac{13}{2} + \frac{3}{2} \ln \frac{\mu^2}{Q^2} \right) \ln \frac{\mu^2}{Q^2} \right\} \\
&\quad \left. + \frac{N_f}{16\pi^2} \left( \frac{\alpha_s(\mu^2)}{\pi} \right)^2 \left[ \frac{128}{3} - 32\zeta(3) \right], \right. \tag{14}
\end{aligned}$$

$$\begin{aligned}
C_m^A(Q^2, \mu^2) &= \frac{1}{4\pi^2} \left[ -6 + \frac{\alpha_s(\mu^2)}{\pi} \left( -12 - 12 \ln \frac{\mu^2}{Q^2} \right) \right. \\
&\quad + \left( \frac{\alpha_s(\mu^2)}{\pi} \right)^2 \left\{ -\frac{4681}{24} + \frac{55}{12} N_f - \left( 34 - \frac{8}{3} N_f \right) \zeta(3) + 115\zeta(5) \right. \\
&\quad \left. - \left( 47 + 12 \ln \frac{\mu^2}{Q^2} \right) \ln \frac{\mu^2}{Q^2} - \left( 11 - \frac{2}{3} N_f \right) \left( \frac{11}{2} + \frac{3}{2} \ln \frac{\mu^2}{Q^2} \right) \ln \frac{\mu^2}{Q^2} \right\} \\
&\quad \left. + \frac{N_f}{16\pi^2} \left( \frac{\alpha_s(\mu^2)}{\pi} \right)^2 \left[ \frac{128}{3} - 32\zeta(3) \right]. \right. \tag{15}
\end{aligned}$$

We ignore terms of  $\mathcal{O}(m^4)$  and higher.

The OPE corrections of the form  $\langle O^{(n)} \rangle / Q^n$  start from the dimension-four operators  $m\bar{q}q$  and  $(\alpha_s/\pi)GG$ . Their Wilson coefficients  $C_{\bar{q}q}^J(Q^2)$  and  $C_{GG}(Q^2)$  are known to  $\mathcal{O}(\alpha_s^2)$  and to  $\mathcal{O}(\alpha_s)$ , respectively, as [21]

$$\begin{aligned}
C_{\bar{q}q}^{V/A}(Q^2) &= -2 \frac{\alpha_s(\mu^2)}{\pi} \left[ 1 + \frac{1}{24} \frac{\alpha_s(\mu^2)}{\pi} \left\{ (116 - 4N_f) + (66 - 4N_f) \ln \frac{\mu^2}{Q^2} \right\} \right] \\
&\quad + / - 2 \left[ 1 + \frac{4}{3} \frac{\alpha_s(\mu^2)}{\pi} + \frac{4}{3} \left( \frac{\alpha_s(\mu^2)}{\pi} \right)^2 \left\{ \left( \frac{191}{24} - \frac{7}{36} N_f \right) + \left( \frac{11}{4} - \frac{1}{6} N_f \right) \ln \frac{\mu^2}{Q^2} \right\} \right] \\
&\quad + \frac{N_f}{3} \left( \frac{\alpha_s(\mu^2)}{\pi} \right)^2 \left( 4\zeta(3) - 3 + \ln \frac{\mu^2}{Q^2} \right) + 0/4, \tag{16}
\end{aligned}$$

$$C_{GG}(Q^2) = \frac{1}{12} \left[ 1 - \frac{11}{18} \frac{\alpha_s(Q)}{\pi} \right]. \tag{17}$$

Here we note that the ‘‘gluon condensate’’  $\langle (\alpha_s/\pi)GG \rangle$  is defined only through the perturbative expression like (12). Due to an operator mixing with the identity operator, the operator  $(\alpha_s/\pi)GG$  contains a quartic power divergence that cannot be unambiguously subtracted within perturbation theory, which is known as the renormalon ambiguity [22]. Therefore, the term  $\langle (\alpha_s/\pi)GG \rangle$  in (12) only has a meaning of a parameter in OPE, that may depend on the order of the perturbative expansion, for instance.

The quark condensate  $\langle \bar{q}q \rangle$  is, on the other hand, well-defined in the massless limit, since it does not mix with lower dimensional operators, provided that the chiral symmetry is

preserved on the lattice. Power divergence may appear at finite quark mass as  $ma^{-2}$ . In the OPE formula (12), it thus leads to a functional dependence  $m^2a^{-2}/Q^4$ . Since the quark mass in the lattice unit is small (0.015–0.050) and  $(aQ)^2$  is of  $O(1)$  in our lattice setup, this divergent contribution is tiny ( $\sim 0.1$ – $0.2\%$ ). In fact, we do not find any significant  $m^2$  dependence in the lattice data. We therefore neglect this  $m^2$  dependence in the numerical analysis.

## B. $V - A$ channel

In addition to the individual vector and axial-vector correlators, we consider the  $V - A$  vacuum polarization function. For the difference  $\Pi_{V-A}^{(0+1)}(Q) \equiv \Pi_V^{(0+1)}(Q) - \Pi_A^{(0+1)}(Q)$ , the lattice data are more precise than the individual  $\Pi_J^{(0+1)}(Q)$ , so that the  $1/Q^6$  and  $1/Q^8$  terms are also necessary:

$$\begin{aligned} \Pi_{V-A}^{(0+1)} \Big|_{\text{OPE}}(Q^2) &= (C_m^V - C_m^A)(Q^2) \frac{1}{Q^2} + (C_{\bar{q}q}^V - C_{\bar{q}q}^A)(Q^2) \frac{\langle m\bar{q}q \rangle}{Q^4} \\ &+ \left( a_6(\mu) + b_6(\mu) \ln \frac{Q^2}{\mu^2} + c_6 m_q \right) \frac{1}{Q^6} + \frac{a_8}{Q^8}. \end{aligned} \quad (18)$$

In the  $V - A$  combination the coefficients  $C_m^V - C_m^A$  and  $C_{\bar{q}q}^V - C_{\bar{q}q}^A$  start at  $\mathcal{O}(\alpha_s)$ . The coefficients  $a_6(\mu)$  and  $b_6(\mu)$  contain dimension six operators  $O_8$  and  $O_1$  as [9, 10]

$$a_6(\mu) = 2\pi \langle \alpha_s O_8 \rangle(\mu) + \frac{2}{5} 4 \langle \alpha_s^2 O_8 \rangle(\mu) + 2 \langle \alpha_s^2 O_1 \rangle(\mu), \quad (19)$$

$$b_6(\mu) = -\langle \alpha_s^2 O_8 \rangle(\mu) + \frac{8}{3} \langle \alpha_s^2 O_1 \rangle(\mu), \quad (20)$$

and the definition of these operators is given by

$$\langle O_8 \rangle = \sum_{\mu, i, j} \langle (\bar{q}_i \gamma_\mu \tau_{ij}^3 q_j)(\bar{q}_i \gamma_\mu \tau_{ij}^3 q_j) - (\bar{q}_i \gamma_\mu \gamma_5 \tau_{ij}^3 q_j)(\bar{q}_i \gamma_\mu \gamma_5 \tau_{ij}^3 q_j) \rangle, \quad (21)$$

$$\langle O_1 \rangle = \sum_{\mu, a, i, j} \langle (\bar{q}_i \gamma_\mu \lambda^a \tau_{ij}^3 q_j)(\bar{q}_i \gamma_\mu \lambda^a \tau_{ij}^3 q_j) - (\bar{q}_i \gamma_\mu \gamma_5 \lambda^a \tau_{ij}^3 q_j)(\bar{q}_i \gamma_\mu \gamma_5 \lambda^a \tau_{ij}^3 q_j) \rangle, \quad (22)$$

with generator matrices  $\tau^3$  and  $\lambda^a$  of flavor SU(2) and color SU(3) symmetries, respectively. The numerical coefficients in the definition of  $a_6$  and  $b_6$  correspond to those of the Naive Dimensional Regularization (NDR) of  $\gamma_5$ .

Unlike the dimension-four quark condensate  $\langle m\bar{q}q \rangle$ ,  $\langle O_8 \rangle$  and  $\langle O_1 \rangle$  remain finite in the massless limit, hence gives leading contribution. The term  $c_6$ , which has a mass-dimension five, describes their dependence on the quark mass. The term  $a_8/Q^8$  represents the contributions from dimension-eight operators.

## IV. FITTING RESULTS

### A. Fit parameters

In the fitting of the lattice data with the functions (12) and (18), we fix the scale  $\mu$  to 2 GeV. We use the value of the quark condensate obtained from a simulation in the  $\epsilon$ -regime using the same lattice formulation at slightly smaller lattice spacing,  $\langle\bar{q}q\rangle(2\text{ GeV}) = -[0.251(7)(11)\text{ GeV}]^3$  [23]. (The values quoted in [12, 24, 25] are slightly different from but consistent with this number. The precise value does not affect the fit much, since the contribution of the  $C_{\bar{q}q}$  term is sub-dominant.) The quark mass is renormalized in the  $\overline{\text{MS}}$  scheme using the non-perturbative matching factor  $Z_m(2\text{ GeV}) = 0.838(17)$  [12] as  $m(\mu) = Z_m(\mu)m_q$ . The coupling constant  $\alpha_s(\mu)$  is transformed to the scale of two-flavor QCD,  $\Lambda_{\overline{\text{MS}}}^{(2)}$ , using the four-loop formula [26]

$$\frac{\alpha_s(\mu^2)}{\pi} = \frac{1}{\beta_0 L} \left[ 1 - \frac{\beta_1 \ln L}{\beta_0^2 L} + \frac{1}{\beta_0^2 L^2} \left\{ \frac{\beta_1^2}{\beta_0^2} (\ln^2 L - \ln L - 1) + \frac{\beta_2}{\beta_0} \right\} + \frac{1}{\beta_0^3 L^3} \left\{ \frac{\beta_1^3}{\beta_0^3} \left( -\ln^3 L + \frac{5}{2} \ln^2 L + 2 \ln L - \frac{1}{2} \right) - 3 \frac{\beta_1 \beta_2}{\beta_0^2} \ln L + \frac{\beta_3}{2\beta_0} \right\} \right] \quad (23)$$

with

$$\beta_0 = \frac{1}{4} \left( 11 - \frac{2}{3} N_f \right), \quad (24)$$

$$\beta_1 = \frac{1}{4^2} \left( 102 - \frac{38}{3} N_f \right), \quad (25)$$

$$\beta_2 = \frac{1}{4^3} \left( \frac{2857}{2} - \frac{5033}{18} N_f + \frac{325}{54} N_f^2 \right), \quad (26)$$

$$\beta_3 = \frac{1}{4^4} \left[ \frac{149753}{6} + 3564\zeta(3) - \left( \frac{1078361}{162} + \frac{6508}{27}\zeta(3) \right) N_f + \left( \frac{50065}{162} + \frac{6472}{81}\zeta(3) \right) N_f^2 + \frac{1093}{729} N_f^3 \right], \quad (27)$$

and  $L = \ln(\mu^2/\Lambda_{\overline{\text{MS}}}^{(N_f)^2})$ .

Then, the free parameters in the fit are the scheme-dependent constant  $c$ , the gluon condensate parameter  $\langle(\alpha_s/\pi)GG\rangle$ , and the QCD scale  $\Lambda_{\overline{\text{MS}}}^{(2)}$  for the fit of an average  $\Pi_{V+A}^{(0+1)}(Q) \equiv \Pi_V^{(0+1)}(Q) + \Pi_A^{(0+1)}(Q)$ . For the difference  $\Pi_{V-A}^{(0+1)}(Q)$ ,  $\Lambda_{\overline{\text{MS}}}^{(2)}$  obtained above is used as an input and the dimension-six condensates  $a_6$ ,  $b_6$  and  $c_6$  are free parameters.

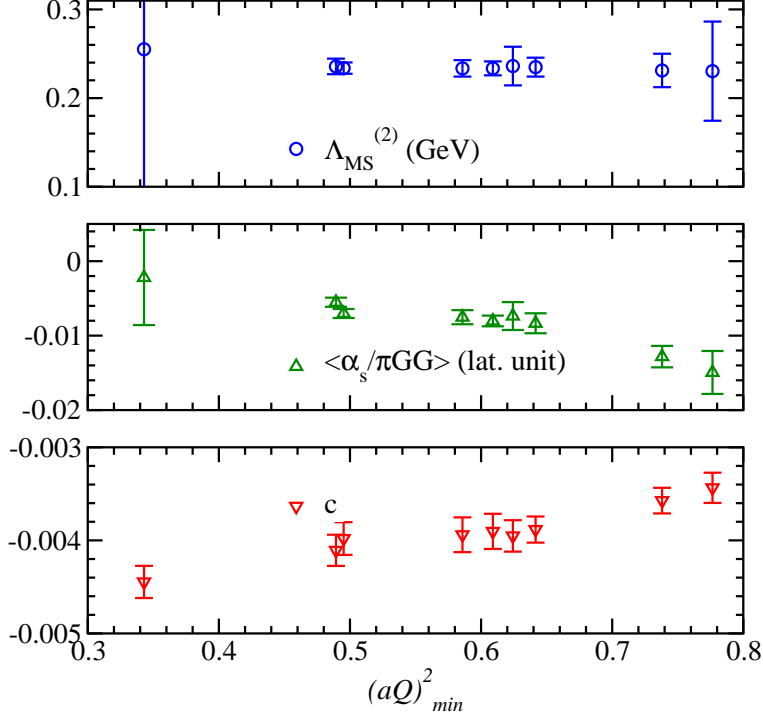


FIG. 4: Fit range dependence of  $\Lambda_{\overline{MS}}^{(2)}$ ,  $\langle(\alpha_s/\pi)GG\rangle$  and the constant term  $c$ . The maximum momentum squared  $(aQ)_{max}^2$  is 1.324.

### B. $V + A$ channel

The OPE analysis requires a window in  $Q^2$  where the systematic errors are under control. The upper limit  $(aQ)_{max}^2 \simeq 1.3238$  is set by taking the points where different definitions of the lattice momentum, *i.e.*  $Q_\mu = (2/a) \sin(\pi n_\mu/L_\mu)$  and  $Q_\mu = (2/a)\pi n_\mu/L_\mu$ , give consistent results within one standard deviation. In the physical unit, this corresponds to 1.92 GeV. To determine  $(aQ)_{min}^2$ , we investigate the dependence of the fit parameters on  $(aQ)_{min}^2$  in Figure 4. We observe that the results for  $\Lambda_{\overline{MS}}^{(2)}$ ,  $\langle(\alpha_s/\pi)GG\rangle$ , and  $c$  are stable between  $(aQ)_{min}^2 \simeq 0.48$  and  $0.65$ , which correspond to the momentum scale 1.16–1.35 GeV. Above  $(aQ)_{min}^2 \simeq 0.65$  the fit becomes unstable; the results are still consistent within one standard deviation.

Figure 5 shows the lattice data for  $\Pi_{V+A}^{(0+1)}(Q)$  at each quark mass and corresponding fit curves. It is clear that the  $Q^2$  dependence of the lattice data is well reproduced by the analytic formula. The quark mass dependence of  $\Pi_{V+A}^{(0+1)}(Q)$  is, on the other hand, not substantial as expected from the fit function (12). Our fit with the known value of  $\langle\bar{q}q\rangle$

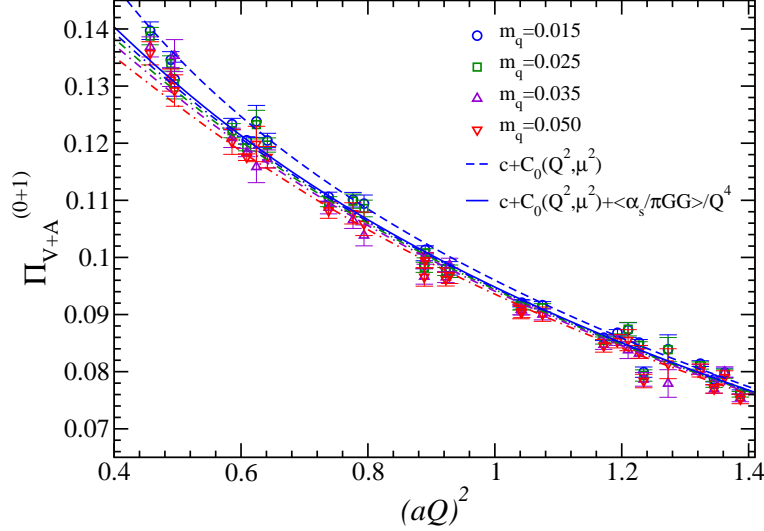


FIG. 5:  $\Pi_{V+A}^{(0+1)}(Q)$  as a function of  $(aQ)^2$ . The lattice data at different quark masses are shown by open symbols. Fit curves for each quark mass and in the chiral limit are drawn. The full result in the chiral limit (dashed-dots curves are at the finite masses, and solid curve is in the chiral limit), as well as that without  $\langle \alpha_s G^2 \rangle / Q^4$  term (dashed curve), are shown.

reproduces the data well. In the chiral limit, (12) is controlled by two parameters:  $\Lambda_{\overline{MS}}^{(2)}$  and  $\langle (\alpha_s/\pi)GG \rangle$  (apart from the unphysical constant term  $c$ ). The fit result in the chiral limit is drawn by a solid curve. The dashed curve drifting upwards towards low  $Q^2$  region shows the result when the contribution from the  $\langle (\alpha_s/\pi)GG \rangle$  term is omitted by hand. It indicates that the  $Q^2$  dependence is mainly controlled by the perturbative piece while the dimension-four term gives a minor contribution, which becomes slightly more important in the low  $Q^2$  regime. Numerically, we obtain  $\Lambda_{\overline{MS}}^{(2)} = 0.234(9)$  GeV and  $\langle (\alpha_s/\pi)GG \rangle = -0.058(7)$  GeV<sup>4</sup> from a global fit of the lattice data at four different quark masses. The fit range of  $(aQ)^2$  is [0.65, 1.3238].

Figure 6 shows  $\Lambda_{\overline{MS}}^{(2)}$  extracted from the lattice data at each quark mass. The flat behavior provides another evidence that the lattice data are consistent with the perturbative prediction (12).



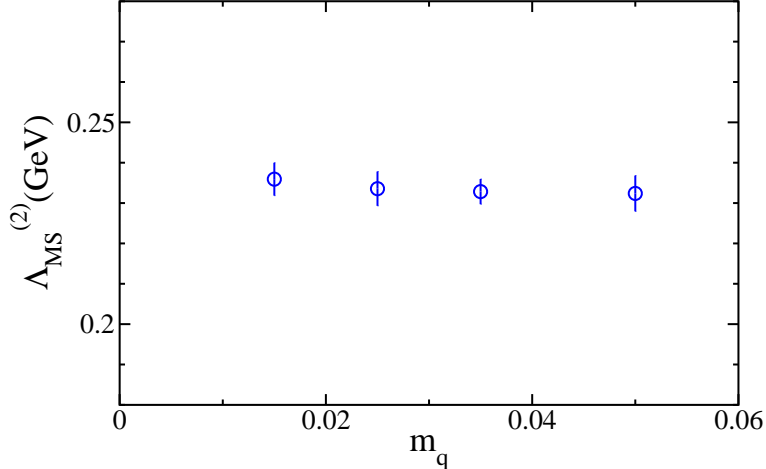


FIG. 6:  $\Lambda_{MS}^{(2)}$  from the data at each quark mass.

### C. Systematic errors

In this subsection we discuss on possible systematic errors in this determination of  $\Lambda_{MS}^{(2)}$ . That includes an estimate of the discretization effects and that of the truncation of perturbative and operator product expansions.

As indicated from the perturbative analysis presented in Section II C, the discretization effects are estimated reasonably well using the perturbation theory. Here, we discuss on the one-loop results for  $\Pi_J(Q)$  on the lattice for our choice of the fermion action and the current operators. This aims at estimating the remaining systematic errors due to the discretization effects after explicitly subtracting the  $B_n^J(Q)$  and  $C_{mn}^J(Q)$  terms.

We again calculate the same one-loop vacuum polarization diagram at representative values of  $(aQ)^2$  between 0.1 and 2.0. After subtracting the  $B_{1,2}^J(Q)$  and  $C_{11}^J(Q)$  terms determined perturbatively in Section II C we numerically obtain the piece corresponding to  $\Pi_J(Q)$ , which contains the physical logarithmic dependence  $-1/(4\pi)^2 \ln((aQ)^2)$  as well as the lattice artifacts. In the continuum theory (or the perturbative calculation with the dimensional regularization, to be specific) only this logarithmic term appears, hence we may identify the remaining terms as the lattice artifacts. They are parametrized by a polynomial of  $(aQ)^2$ .

The result of the one-loop calculation is shown in Figure 7 (upper panel). We fit the data with a function including the known logarithmic term plus a quadratic function of  $(aQ)^2$  and

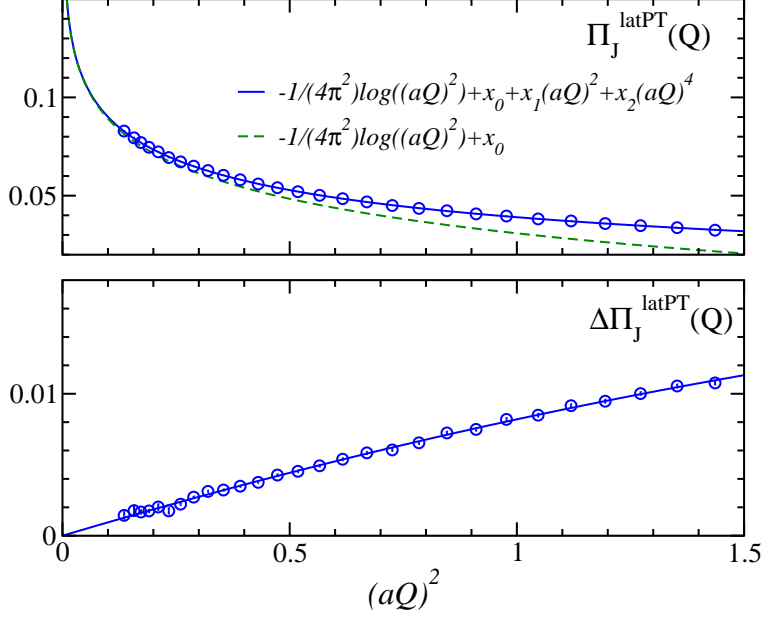


FIG. 7: One-loop calculation of  $\Pi_V(Q)$  (upper panel) at representative values of  $(aQ)^2$  (circles) and a fit with the log-plus-polynomial form. The dashed curve shows the purely logarithmic contribution. The term that represents the lattice artifact  $\Delta\Pi_V(Q)$  is shown in the lower panel.

obtain the numerical result  $\Pi_V^{\text{LatPT}}(Q^2) = -\frac{1}{4\pi^2} \ln((aQ)^2) + 0.03085(9) + 0.00952(30)(aQ)^2 - 0.00132(20)(aQ)^4$ .

In order to estimate the impact of this size of the discretization effect, we add this term to the fit function (12) and repeat the whole analysis. The result is  $\Lambda_{\overline{MS}}^{(2)} = 0.249(37)$  GeV and  $\langle(\alpha_s/\pi)GG\rangle = +0.11(15)$  GeV<sup>4</sup>. We find that  $\Lambda_{\overline{MS}}^{(2)}$  is not largely affected, while  $\langle(\alpha_s/\pi)GG\rangle$  is very sensitive to the lattice artifact and in fact changes its sign.

Other (Lorentz-violating) discretization effects due to  $B_n^J(Q)$  and  $C_{mn}^J(Q)$  are subtracted non-perturbatively so that the associated error should be negligible. With our preliminary calculation of the above mentioned conserved vector and axial-vector currents for the overlap fermion, we confirmed that the results are consistent with the calculation presented in this paper obtained with the non-conserved currents (3) and (4) up to the unphysical constant term  $c$ . This observation confirms that our procedure to subtract the  $B_n^J(Q)$  and  $C_{mn}^J(Q)$  terms is working as expected.

The truncation of the perturbative and operator product expansions is also a possible source of the systematic error. In order to estimate the size of the former, we repeat the

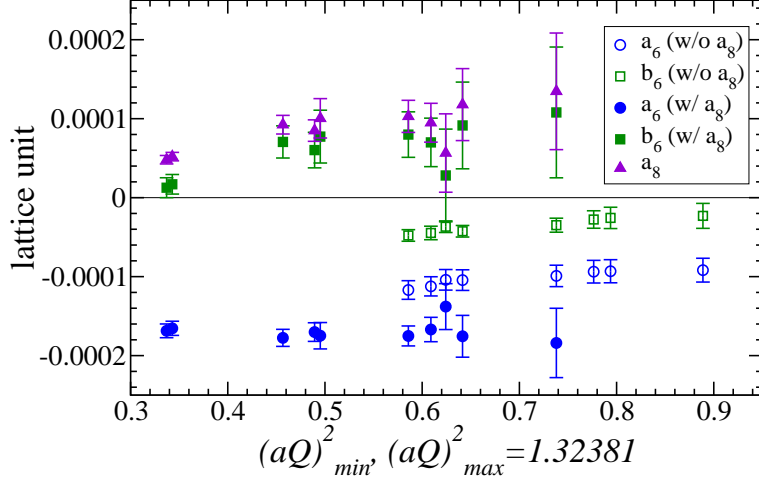


FIG. 8: Fit range dependence of  $a_6(\mu)$ ,  $b_6(\mu)$  and  $a_8$ . The horizontal axis denotes the minimum momentum squared  $(aQ)_{\min}^2$ .

analysis using the fit formulae truncated at a lower order (two-loop level), and find that the change of  $\Lambda_{\overline{MS}}^{(2)}$  is much less than one standard deviation. It indicates that the higher order effects are negligible. The error from the truncation of OPE is estimated by dropping the terms of  $\mathcal{O}(1/Q^4)$  from (12). From fits with higher  $(aQ)_{\min}^2$  (between 0.79 and 0.89) to avoid contamination from the  $1/Q^4$  effects, we obtain  $\Lambda_{\overline{MS}}^{(2)} = 0.247(3)$  GeV. The deviation of  $\Lambda_{\overline{MS}}^{(2)}$  is about the same size as that due to the discretization effect.

The errors due to finite physical volume and the fixed topological charge in our simulation [27] are unimportant for the short-distance quantities considered in this work. A simple order counting gives an error of order  $1/(QL)^2 \lesssim 0.4\%$  or smaller.

To quote the final result, we take the central value from the fit without the discretization effect

$$\Lambda_{\overline{MS}}^{(2)} = 0.234(9)_{-0}^{+16} \text{ GeV}, \quad (28)$$

where the first error is statistical and the second is systematic due to the discretization and truncation errors. The result is compatible with previous calculations of  $\alpha_s$  in two-flavor QCD:  $\Lambda_{\overline{MS}}^{(2)} = 0.250(16)(16)$  GeV [28] and  $0.249(16)(25)$  GeV [29]. (The physical scale is normalized with an input  $r_0 = 0.49$  fm.)

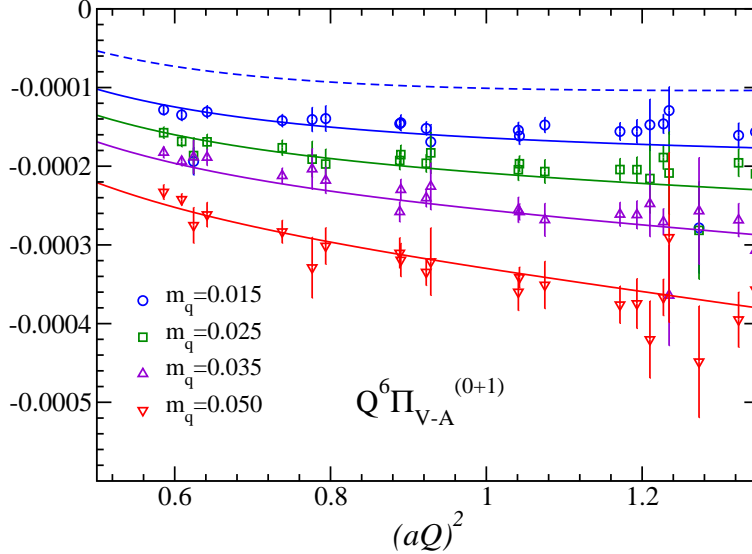


FIG. 9:  $Q^6 \Pi_{V-A}^{(0+1)}(Q)$  as a function of  $(aQ)^2$ . The lattice data at different quark masses are shown by open symbols. Fit curves for each quark mass and in the chiral limit are drawn.

#### D. $V - A$ channel

For the fit of the  $V - A$  vacuum polarization  $\Pi_{V-A}^{(0+1)}(Q)$ , we also examine the fit range dependence. In Figure 8 the fit parameters  $a_6$ ,  $b_6$  and  $a_8$  are shown as a function of  $(aQ)_{\min}^2$  while fixing  $(aQ)_{\max}^2$  at the same value 1.3238. We attempt to fit with (filled symbols) and without (open symbols) the  $a_8/Q^8$  term in order to investigate how stable the results are against the change of the order of the  $1/Q^2$  expansion. We find that the fit with  $a_8/Q^8$  is stable down to  $(aQ)_{\min}^2 \simeq 0.46$ , while the other could not be extended below  $(aQ)_{\min}^2 \simeq 0.58$ . The difference between filled and open symbols is marginal for  $a_6$  (circles), but too large to make a reliable prediction for  $b_6$  (squares). To quote the results we set  $(aQ)_{\min}^2 = 0.586$  for both  $\Pi_{V+A}^{(0+1)}(Q)$  and  $\Pi_{V-A}^{(0+1)}(Q)$ .

In Figure 9, we plot  $Q^6 \Pi_{V-A}^{(0+1)}(Q)$  as a function of  $(aQ)^2$  for four different values of the quark mass  $m_q$ . The quark mass dependence is clearly observed. The main contribution comes from a dimension-six term  $c_6 m_q / Q^6$ , while the dimension-four term  $\langle m \bar{q} q \rangle / Q^4$  is subdominant ( $\sim 20\%$ ), as its coefficient starts at  $\mathcal{O}(\alpha_s)$ . In the chiral limit, there is a small but non-zero value remaining in  $Q^6 \Pi_{V-A}^{(0+1)}|_{\text{OPE}}(Q^2)$  as shown by a dashed curve in the plot. This is due to the four-quark condensates  $a_6$  and  $b_6$ .

The four-quark condensate  $a_6$  obtained from  $\Pi_{V-A}^{(0+1)}(Q)$  is

$$a_6(2 \text{ GeV}) = -0.0038(3) \binom{+16}{-0} \text{ GeV}^6, \quad (29)$$

where the first error is statistical. The second error represents an uncertainty due to the truncation of the  $1/Q^2$  expansion. The central value is taken from the fit with  $a_8/Q^8$  in (18) and the error reflects the shift when this term is discarded. The result agrees with the previous phenomenological estimates  $-(0.003 \sim 0.009) \text{ GeV}^6$  [30]. The other condensate is less stable; we obtain  $b_6(2 \text{ GeV}) = +0.0017(7) \text{ GeV}^6$  or  $-0.0008(2) \text{ GeV}^6$  with or without the  $\mathcal{O}(1/Q^8)$  term, respectively.

## V. CONCLUSION

Many of the lattice calculations to date have analyzed the two-point correlation functions to extract physical quantities such as the hadron mass spectra and decay constants. Usually the exponential fall-off of the correlator at large Euclidean time separation is used to isolate the ground state contribution. In this way, however, many interesting pieces of information are lost. They are in the short and middle distance regime where the perturbative analysis is also applicable. We use the two-point current correlators calculated on the lattice to extract the strong coupling constant with the help of the continuum perturbation theory and the operator product expansion. The recent work by Allison *et al.* has exploited [5] the similar idea and applied it to the charmonium correlator to extract the charm quark mass and the strong coupling constant.

With the exact chiral symmetry realized by the overlap fermion formulation, the analysis of the lattice data is simplified. For the case of the vacuum polarizations, the continuum form of OPE may be applied without suffering from additional operator mixings, such as the additive renormalization of the operator  $\bar{q}q$ , which appears in the Wilson-type fermion formulations. We also obtain the four-quark condensates  $a_6$  and  $b_6$ , which are relevant to the analysis of kaon decays [9].

In principle, our analysis does not require lattice perturbation theory, which is too complicated to carry out to the loop orders available in the continuum theory. But the perturbative calculation is still useful to estimate the discretization effects, which is well-described by perturbation theory in the asymptotic free theories.

The result for the strong coupling constant is compatible with previous lattice calculations. The size of statistical and systematic errors is also comparable with them. An obvious extension of this work is the calculation in 2+1-flavor QCD, which is underway [31]. We also study the improvement of the analysis by using the conserved current for the overlap fermion formulation.

### Acknowledgments

Numerical calculations are performed on IBM System Blue Gene Solution and Hitachi SR11000 at High Energy Accelerator Research Organization (KEK) under a support of its Large Scale Simulation Program (No. 07-16). This work is supported by the Grant-in-Aid of the Japanese Ministry of Education (No. 18034011, 18340075, 18740167, 19540286, 19740121, 19740160, 20025010, 20340047, 20740156), and National Science Council of Taiwan (No. NSC96-2112-M-002-020-MY3, NSC96-2112-M-001-017-MY3).

- 
- [1] M. Davier, A. Hocker and Z. Zhang, *Rev. Mod. Phys.* **78**, 1043 (2006) [arXiv:hep-ph/0507078].
  - [2] E. V. Shuryak, *Rev. Mod. Phys.* **65**, 1 (1993).
  - [3] T. Blum, *Phys. Rev. Lett.* **91**, 052001 (2003) [arXiv:hep-lat/0212018].
  - [4] M. Gockeler, R. Horsley, W. Kurzinger, D. Pleiter, P. E. L. Rakow and G. Schierholz [QCDSF Collaboration], *Nucl. Phys. B* **688**, 135 (2004) [arXiv:hep-lat/0312032].
  - [5] I. Allison *et al.*, *Phys. Rev. D* **78**, 054513 (2008), [arXiv:0805.2999 [hep-lat]].
  - [6] S. L. Adler, *Phys. Rev. D* **10**, 3714 (1974).
  - [7] L. R. Surguladze and M. A. Samuel, *Phys. Rev. Lett.* **66**, 560 (1991) [Erratum-ibid. **66**, 2416 (1991)].
  - [8] S. G. Gorishnii, A. L. Kataev and S. A. Larin, *Phys. Lett. B* **259**, 144 (1991).
  - [9] J. F. Donoghue and E. Golowich, *Phys. Lett. B* **478**, 172 (2000) [arXiv:hep-ph/9911309].
  - [10] V. Cirigliano, E. Golowich and K. Maltman, *Phys. Rev. D* **68**, 054013 (2003) [arXiv:hep-ph/0305118].
  - [11] S. Aoki *et al.* [JLQCD Collaboration], *Phys. Rev. D* **78**, 014508 (2008) [arXiv:0803.3197 [hep-lat]].

- [12] J. Noaki *et al.* [JLQCD and TWQCD Collaborations], Phys. Rev. Lett. **101**, 202004 (2008) arXiv:0806.0894 [hep-lat].
- [13] H. Neuberger, Phys. Lett. B **417**, 141 (1998) [arXiv:hep-lat/9707022].
- [14] H. Neuberger, Phys. Lett. B **427**, 353 (1998) [arXiv:hep-lat/9801031].
- [15] M. Luscher, Phys. Lett. B **428**, 342 (1998) [arXiv:hep-lat/9802011].
- [16] P. H. Ginsparg and K. G. Wilson, Phys. Rev. D **25**, 2649 (1982).
- [17] Y. Kikukawa and A. Yamada, Nucl. Phys. B **547**, 413 (1999) [arXiv:hep-lat/9808026].
- [18] E. Shintani *et al.* [JLQCD Collaboration], PoS **LAT2007**, 134 (2007) [arXiv:0710.0691 [hep-lat]].
- [19] E. Shintani *et al.* [JLQCD Collaboration], Phys. Rev. Lett. **101**, 242001 (2008), arXiv:0806.4222 [hep-lat].
- [20] M. A. Shifman, A. I. Vainshtein and V. I. Zakharov, Nucl. Phys. B **147**, 385 (1979).
- [21] K. G. Chetyrkin, V. P. Spiridonov and S. G. Gorishnii, Phys. Lett. B **160**, 149 (1985).
- [22] G. Martinelli and C. T. Sachrajda, Nucl. Phys. B **478**, 660 (1996) [arXiv:hep-ph/9605336].
- [23] H. Fukaya *et al.* [JLQCD Collaboration], Phys. Rev. Lett. **98**, 172001 (2007) [arXiv:hep-lat/0702003].
- [24] H. Fukaya *et al.* [JLQCD and TWQCD collaborations], Phys. Rev. D **76**, 054503 (2007) [arXiv:0705.3322 [hep-lat]].
- [25] H. Fukaya *et al.* [JLQCD collaboration], Phys. Rev. D **77**, 074503 (2008) [arXiv:0711.4965 [hep-lat]].
- [26] T. van Ritbergen, J. A. M. Vermaseren and S. A. Larin, Phys. Lett. B **400**, 379 (1997) [arXiv:hep-ph/9701390].
- [27] S. Aoki, H. Fukaya, S. Hashimoto and T. Onogi, Phys. Rev. D **76**, 054508 (2007) [arXiv:0707.0396 [hep-lat]].
- [28] M. Della Morte, R. Frezzotti, J. Heitger, J. Rolf, R. Sommer and U. Wolff [ALPHA Collaboration], Nucl. Phys. B **713**, 378 (2005) [arXiv:hep-lat/0411025].
- [29] M. Gockeler, R. Horsley, A. C. Irving, D. Pleiter, P. E. L. Rakow, G. Schierholz and H. Stuben, Phys. Rev. D **73**, 014513 (2006) [arXiv:hep-ph/0502212].
- [30] A. A. Almasy, K. Schicher and H. Spiesberger, [arXiv:0802.0980[hep-lat]] and references therein.
- [31] S. Hashimoto *et al.* [JLQCD collaboration], PoS **LAT2007**, 101 (2007) [arXiv:0710.2730 [hep-

lat]].